

Long Electron–Hole Separation of ZnO–CdS Core–Shell Quantum Dots

Fen Xu,[†] Vyacheslav Volkov,[‡] Yimei Zhu,[‡] Hanying Bai,[†] Anthony Rea,[§] Nikesh V. Valappil,[§] Wei Su,[†] Xueyun Gao,[†] Igor L. Kuskovsky,^{*,§} and Hiroshi Matsui^{*,†}

Department of Chemistry and Biochemistry, The City University of New York - Hunter College, 695 Park Avenue, New York, New York 10065, Brookhaven National Laboratory (BNL), CMP Materials Science Department, Upton, New York 11973, and Department of Physics, The City University of New York - Queens College, Flushing, New York 11367

Received: April 25, 2009; Revised Manuscript Received: September 2, 2009

The tunability of electronic and optical properties of semiconductor nanocrystal quantum dots (QDs) has been an important subject in nanotechnology. While control of the emission property of QDs in wavelength has been studied extensively, control of the emission lifetime of QDs has not been explored in depth. In this report, ZnO–CdS core–shell QDs were synthesized in a two-step process, in which we initially synthesized ZnO core particles, and then stepwise slow growth of CdS shells followed. The coating of a CdS shell on a ZnO core increased the exciton lifetime more than 100 times that of the core ZnO QD, and the lifetime was further extended as the thickness of shell increased. This long electron–hole recombination lifetime is due to a unique staggered band alignment between the ZnO core and CdS shell, so-called type II band alignment, where the carrier excitation holes and electrons are spatially separated at the core and shell, and the exciton lifetime becomes extremely sensitive to the thickness of the shell. Here, we demonstrated that the emission lifetime becomes controllable with the thickness of the shell in ZnO–CdS core–shell QDs. The longer excitonic lifetime of type II QDs could be beneficial in fluorescence-based sensors, medical imaging, solar cells photovoltaics, and lasers.

Introduction

The tunability of electronic and optical properties of semiconductor nanocrystal quantum dots (QDs) has been an important subject in nanotechnology because of their promising applications in solar cells,¹ light emitters,² biotags,³ and bio-sensing.⁴ To further control these properties precisely, hetero-structured or core–shell QDs have been developed. For example, coatings on CdSe QDs with CdS⁵ or ZnS⁶ shells resulted in greatly enhanced fluorescence quantum yield and photochemical stability due to the electron and hole confinement to the core. While the control of the emission property of QDs in wavelength has been studied extensively, the control of the emission lifetime of QDs has not been explored in depth. While emission lifetime control is difficult for most core–shell QDs, one can slow the recombination between the two carriers if the band structure between the core and the shell materials is staggered and one photogenerated carrier is predominantly confined to the core and the other is located in the shell (Figure 1). In this so-called type II QD system, the longer exciton lifetime arises from the decreased wave function overlaps between holes and electrons, and the emission lifetime becomes extremely sensitive to the thickness of the shell. Here, we demonstrated that indeed the increase of the shell thickness of a ZnO–CdS core–shell QD could increase its exciton lifetime. The longer excitonic lifetime of type II QDs could be beneficial in fluorescence-based sensors, medical imaging, solar cells photovoltaics, and lasers.^{7,8} Furthermore, the type II hetero-

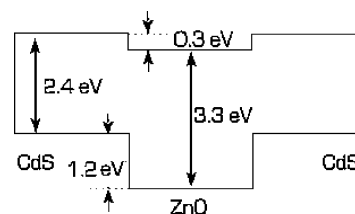


Figure 1. Band diagram of the ZnO–CdS interface.²²

structured QDs suppress the Auger recombination,^{9–11} which is highly desirable for nanoparticle-based optoelectronic devices.^{12,13}

In addition, the number of reports for type II core–shell QD systems with visible absorption and emission is relatively small,^{14–19} and it is very useful to increase the lineups of core–shell type II QDs, which will enable one to choose desired physical properties such as absorption, emission, and excitonic lifetime in a wide range, so that the type II QDs could be applied more broadly to improve energy storage, photovoltaic devices, and catalysis. To meet this thirst for QD development, we explored type II QDs with ZnO cores for visible absorption. The exciton lifetime of the core–shell ZnO–CdS QDs was at least 100 times greater than the typical type I QDs, and the exciton lifetime further increased as the coating thickness of the CdS shell on a ZnO core increased.

Experimental Section

Synthesis of ZnO–CdS Core–Shell QDs. Trioctylphosphine oxide (TOPO, 90% pure), trioctylphosphine (TOP, 95% pure), and hexadecylamine (HAD, 99% pure) were obtained from Sigma Aldrich and Fluka, respectively. Dimethylcadmium (CdMe₂) and diethylzinc (ZnEt₂) were purchased from Strem and Fluka, respectively, and both chemicals were filtered

* To whom correspondence should be addressed. E-mail: hmatsui@hunter.cuny.edu, Igor.Kuskovsky@qc.cuny.edu.

[†] The City University of New York - Hunter College.

[‡] Brookhaven National Laboratory (BNL).

[§] The City University of New York - Queens College.

separately through a 0.2 μm filter in a glovebox. Hexamethyldisilathiane [(TMS)₂S] was used as purchased from Fluka. Anhydrous hexane and methanol were purchased from Sigma Aldrich. The ZnO core nanoparticles from Zn(Et)₂ were synthesized according to the method previously reported by Guyot-Sionnest and co-workers.²⁰ The zinc precursor solution was prepared in a glovebox by dissolving 150 μL of Zn(Et)₂ in 4 mL of decane and then injected into 4 mL of octylamine degassed by bubbling with O₂ for about 1 h. This mixture was bubbled with O₂ for another 5 min and injected into 6 g of TOPO at 200 °C under N₂ flow and left for 12 h. The reaction mixture was allowed to cool to 160–180 °C for the growth of the ZnO NPs. To grow larger size particles, larger amounts of Zn–O precursors can be added. Adjusting the growth time, controlled by the termination of the reaction upon cooling, was also employed to change the size of ZnO NPs. Then, ZnO NPs were precipitated from the growth solution by adding methanol, and the precipitated ZnO NPs (~100 mg) were dispersed in TOPO (7.5 g) and HDA (4 g) at 100 °C. For the CdS growth around the ZnO core, 150 μL of (TMS)₂S and 35 μL of Cd(Me)₂ were dissolved in 4 mL of TOP in a glovebox, and then this mixture was added drop-wise into the reaction flask containing the ZnO core nanoparticles at 140 °C. This dropwise injection of precursors is very important to slow the ion-exchange reaction between Zn–O ions and Cd–S ions through the surface of ZnO core NPs because the CdS exchange process is so fast that the ZnO core cannot survive without slowing the shell growth reaction. It should also be noted that because of this relatively fast CdS reaction the concentration of ZnO NPs was very sensitive to influencing the yield of the resulting ZnO–CdS core–shell QDs. Then, the resulting core–shell QDs were annealed at 110 °C for 24 and 48 h, while the annealing time between 24 and 48 h did not make a significant difference in the emission properties of the resulting crystals. Obtained QDs were precipitated by adding methanol and dispersed in hexane for further optical measurements. This two-step coating approach was effective to avoid the formation of alloyed nanoparticles at 200–240 °C.²¹ The use of these organometallic precursors also assisted robust nucleations of the core and shell to decompose them at a relatively low temperature.

Analysis of QDs. HRTEM images and SAED patterns were recorded with a JEOL3000F microscope operating at 300 keV, equipped with a field emission gun and installed at Brookhaven National Laboratory. Point resolution of the JEOL3000F microscope is ~1.55 Å. Nanoarea EDX analysis was performed using a Thermo Noran EDX system attached to the JEOL3000F microscope. X-ray microanalysis for composition studies at nanoscale was carried out with a Si (Li) detector using a Vantage 2.4 digital pulse processor and Vista 2.3 microanalysis software. Optical absorption (OA) spectra were recorded by a Cary 50 Probe UV–vis spectrophotometer in the wavelength range of 300–600 nm, and photoluminescence (PL) emission spectra were recorded by a Jobin Yvon-Spex Fluorolog spectrophotometer. Time-resolved PL studies were performed with a Jobin Yvon FluoroMax-3, using a time correlated single-photon counting system with a 310 nm nano-LED as an excitation source. This system allows time resolution of <1 ns. All measurements were performed at room temperature.

Results and Discussion

To grow core–shell ZnO–CdS QDs, CdS shells were grown on the ZnO nanoparticles by applying the stepwise reaction processes between (TMS)₂S and CdMe₂. CdS shell growth on the ZnO core could be accomplished by the slow ion-exchange

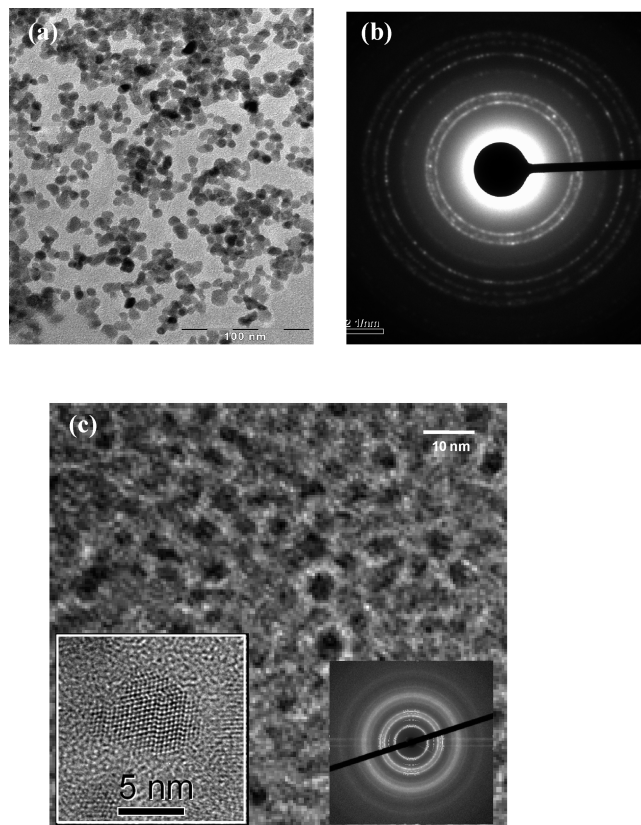


Figure 2. (a) TEM image of ZnO QDs. Scale bar = 100 nm. (b) Electronic diffraction pattern of ZnO QDs. (c) TEM image of ZnO–CdS core–shell QDs. Scale bar = 10 nm. Inset (left): High-resolution TEM image of ZnO–CdS core–shell QDs. Scale bar = 5 nm. Inset (right): Electronic diffraction pattern of ZnO–CdS core–shell QDs.

reaction between ZnO and CdS on the surface of ZnO NPs. Further stabilization of the CdS shell growth was accomplished by exchanging (TMS)₂S with more stable capping agents, octylamine, TOPO, and TOP. The thickness of the CdS shell was controlled by the amount of precursors and subsequent annealing process. The band alignment between the core of ZnO and the shell of CdS is summarized in Figure 1.²² When the photogenerated electrons will be confined within the ZnO core and holes will be located in the CdS shell, their recombination is significantly slowed by this band alignment.

Figure 2a presents the TEM image of ZnO NPs. The average diameter of NPs is 5.0 nm with a standard deviation of 0.4 nm, as measured from calibrated high-magnification TEM images and directly from high-resolution (HR-TEM) lattice images for several dozens of NP groups dispersed on 3 mm diameter Cu-grids for 20 samples. The electron diffraction pattern in Figure 2b reveals that ZnO NPs possess a hexagonal structure as all the diffraction rings could be indexed using a hexagonal lattice. The (hkl) indices of the diffraction rings, starting from internal ring to outside, are matched to (100), (002), (101), (102), (110), (103), and (112) planes of the wurtzite ZnO structure. Figure 2c shows TEM images of ZnO–CdS core–shell QDs, and their average diameter is 5.0 nm. Here, it is interesting to observe that the size of ZnO–CdS core–shell QDs is similar to that of ZnO core NPs. This unchanged size between the core NPs and resulting core–shell QDs could indicate that Cd–S ions replace Zn–O ions by the kinetically controlled substitution ion-exchange reaction at the ZnO core surface to form CdS shells rather than building CdS coating layers over a ZnO core. It

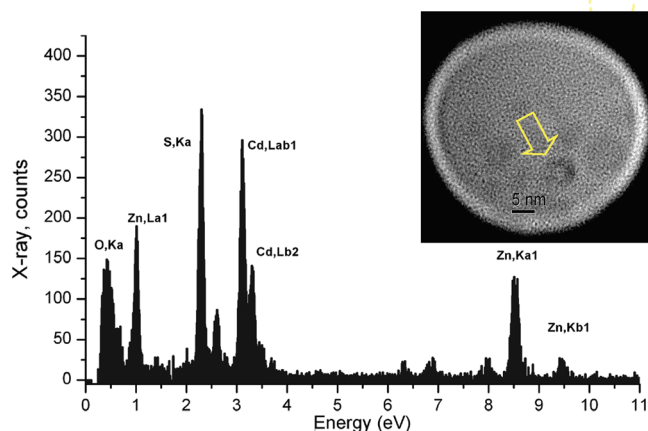


Figure 3. Elemental analysis of ZnO-CdS QDs by energy-dispersive X-ray (EDX) spectroscopy. Inset shows TEM image of a single ZnO-CdS QD (arrow) for the EDX spectrum.

should be noted that the similar replacement of atoms between Cd and Ag was observed in CdSe QDs.²³ The electronic diffraction pattern in the inset of Figure 2c matches most of hexagonal CdS lattice *d*-spacings with a slight lattice shift toward ZnO. This observation supports our hypothesis, and it shows that the crystalline structure of core-shell ZnO-CdS QDs matches the hexagonal CdS, which is not its native structure. Under this hypothesis, it is reasonable that the CdS shell inherits the hexagonal structure of the ZnO core because Cd-S ions replace Zn-O ions of the core where the structure is hexagonal. In the inset of Figure 2c, lattice fringes are clearly observed in the high-resolution TEM images of the core-shell sample, and these fringes persist throughout the entire nanocrystal, indicating the dislocation-free epitaxial growth with full elastic crystalline lattice matching between the core and shell compositions. Because the lattice mismatch between the core and shell is too small in ZnO-CdS QDs to resolve them clearly in HRTEM, in the next paragraphs, these QDs are firmly verified to be neither a homogeneous alloy of CdS and ZnO nor pure hexagonal CdS NPs by their energy disperse X-ray spectrum and photoluminescence lifetime study.

To confirm that these core-shell QDs consist of ZnO and CdS, we analyzed them with local X-ray emission using a EDS Thermo-Noran system, equipped with a X-ray Si(Li) detector attached to a JEOL3000F microscope. Using the smallest condenser aperture, all X-ray data for NPs were acquired in special nanoarea illumination (probe size ~ 20 nm) high-resolution imaging mode, which allowed for HR-TEM imaging and parallel X-ray data recording in a random search for single NPs observed within the focused nanoprobe image (Figure 3).

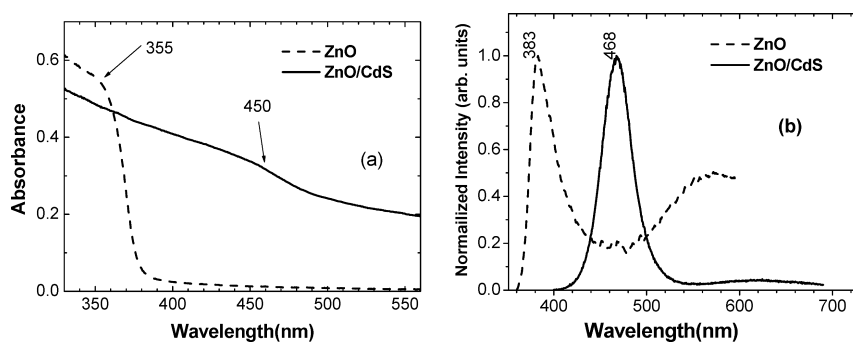


Figure 4. (a) Absorption spectra and (b) photoluminescence spectra of ZnO QDs (solid line) and core-shell ZnO-CdS QDs (dotted line).

The X-ray spectrum shows ZnK $_{\alpha 1}$, ZnK $_{\beta 1}$, OK $_{\alpha}$, SK $_{\alpha}$, CdL $_{\beta 1}$, and CdL $_{\beta 2}$ lines, recorded by using the focused electron beam probe, which represents an accurate result for a single QD. It should be noted that this spectrum is reproducibly consistent among 50 different particles and even with larger QDs formed by aggregating 3–4 NPs. The ratio of peak intensities between Cd-S and Zn-O in this core-shell QD was 1:0.4 on average, determined from relative X-ray peak intensities by using Vista 2.3 microanalysis software and thin correction. This ratio indicates that the CdS shell has a larger size and relative weight as compared to the ZnO core in the QD. The dominant weight of a CdS shell from the X-ray spectrum is consistent with the diffraction pattern for ZnO-CdS QD in Figure 2c, where diffraction is also dominated by the hexagonal CdS-like phase.

While all TEM and EDS results indicate that these QDs consist of a ZnO core and CdS shell, a distinct crystalline boundary between the core and shell is difficult to resolve because of the very small lattice mismatch in homomorphic epitaxial heterostructures between wurtzite ZnO and CdS (<7% in bulk). Therefore, whether the core-shell QDs produce *p-n* heterojunctions for the type II band structure offset or create a random alloy with no band structure offset, can be best addressed by direct optical measurements and exciton lifetime measurements for ZnO-CdS QDs. In Figure 4a, ZnO NPs exhibit typical absorption spectra for type I QDs with an excitonic peak at ~ 355 nm (3.49 eV), and a similar absorption band was observed by other groups.²⁴ When ZnO NPs were coated by CdS shells, the distinctive absorption edge for the type I ZnO cores was replaced by a relatively smooth tail with a small shoulder observed at ~ 450 nm. This is a characteristic spectral signature of the type II QDs because the absorption of type II QDs is effectively suppressed with a peak broadening in their spectra as compared to the type I QDs due to the weaker oscillator strength with a decrease in wave function overlap caused by the indirect spatial nature of long-lived exciton and larger variation of transition energies.²⁵ Therefore, the spectrum of QDs in Figure 4a is consistent with the spectral feature for the characteristic type II QD heterostructure.^{17,19,20,26} The photoluminescence (PL) peak of the core-shell QD appears at 468 nm in Figure 4b, and the PL peak was red-shifted with the thickness of the CdS shell (Supporting Information). If these ZnO NPs were not coated by CdS shells, PL peaks and absorption edges of pure ZnO should have been observed in this spectrum. Therefore, the lack of these combination peaks in Figure 4b also supports the formation of core-shell QDs. For the type II core-shell QDs, the electron-hole recombination energy is significantly reduced because of the core-shell structure (Figure 1), even though the influence of NP size confinement to the band gap energy is taken into account. Therefore, the red shift of the PL peak from 383 to 468 nm is

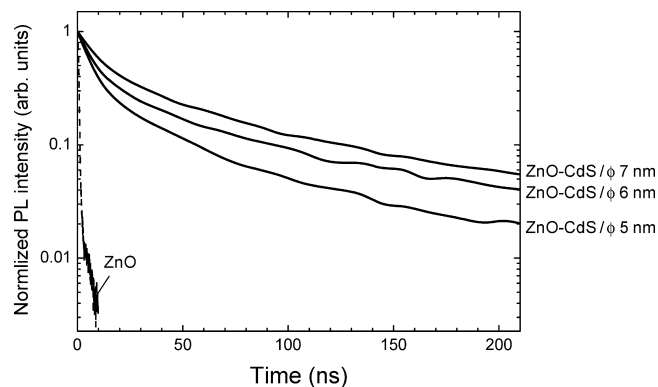


Figure 5. Time-resolved PL decays for pure ZnO and core-shell ZnO-CdS QDs with different QD diameters. CdS shell thickness is proportional to the QD diameter as the core maintains the original size or less during shell growth.

consistent with the core-shell formation. It should be noted that when the CdS precursors were not added to the solution of the core NPs in the dropwise manner and the growth speed of the shell was increased, the PL peak and absorption peak of resulting QDs was shifted back to the 485 and 470 nm, respectively, corresponding to the spectral positions of neat CdS.²⁷ At this point, the ion-exchange reaction between Zn-O and Cd-S was completed under this fast growth condition, and the consumption of the core resulted in producing pure CdS NPs.

As discussed above, in general, for core-shell nanoparticles with a diameter less than 10 nm, the core is very difficult to distinguish from the shell by TEM and diffraction because the lattices of the core and shell are matching very closely. To firmly verify the type II characteristics of this core-shell QD, we compared the PL lifetimes of the ZnO-CdS core-shell QDs with different thicknesses of the CdS shell as shown in Figure 5. The diameter of each core-shell QD is labeled for the corresponding spectrum, and the shell thickness is assumed to proportionally increase with the diameter of the QD as long as the core maintains the original size or less during the shell growth on the core. Typically, the PL lifetime of type II QDs becomes longer as the shell thickness increases due to extended excitonic lifetimes with more discrete charge confinement.¹⁸ In Figure 5, PL lifetimes of ZnO-CdS QDs increase as the CdS shell becomes thicker, and the excitonic lifetime of core-shell QDs with the thickest shell is at least 100 times greater than the neat type I ZnO QD with a lifetime of 1 ns. If the resulting QD is not the core-shell NP, the NP is the type I QD, and its PL lifetime becomes short. However, the excitonic PL lifetime of our QD is on the order of 100 ns; this long lifetime strongly indicates that this NP is the type II QD with a staggered band alignment between the core and shell. Then, the only possible structure for the resulting NP to have the type II characteristics is the hybrid one with ZnO as the core and CdS as the shell. This is also supported by the red shift of the PL peak with an increase in shell thickness as discussed above. It is unlikely that this slow PL lifetime is caused by a defect of the shell because the lifetime changes as a function of shell thickness. This observation of the much longer PL lifetimes of ZnO-CdS QDs also eliminates the possibility that these QDs are alloy of ZnO and CdS with the homogeneous hexagonal crystalline structure because the alloy cannot have the type II characteristics, and then the lifetime should have been as fast as the type I QDs.

Conclusion

The ZnO-CdS type II core-shell QDs were synthesized at relatively low temperature. All HRTEM images, ED patterns, and EDX spectra suggest that these QDs have a heterogeneous ZnO core-CdS shell structure, and analysis from UV-vis absorption spectra, PL spectra, and PL lifetime measurements firmly confirm that these core-shell ZnO-CdS QDs possess the type II band structure offset. The spatial electron-hole separation between the core and shell, greatly enhanced by the type II band structure offset in the ZnO-CdS QD heterostructures, results in the extremely long exciton lifetime. These type II ZnO-CdS QDs can be excited and detected in the visible range, and therefore, these QDs with such long exciton lifetimes could have an advantage to be applied in the fields of photoluminescent markers, medical imaging, photonics, solar cells, nanoelectronics, and biosensors.

Acknowledgment. This work was supported by the U.S. Department of Energy under Award DE-FG-02-01ER45935 and the U.S. DOE, Division of Materials, Office of Basic Energy Science, Contract DE-AC02-98CH10886. Hunter College infrastructure is supported by the National Institutes of Health, the RCMI program (G12-RR003037-245476). F.X. thanks Professor Glen Kowach and Mr. Chunming Feng for the use of the glovebox. H.M. and F.X. also thank Dr. Jorge Morales for the assistance of TEM.

Supporting Information Available: PL spectra of core-shell QDs with the shell thickness change. This material is available free of charge via the Internet at <http://pubs.acs.org>.

References and Notes

- (1) Huynh, W. U.; Peng, X. G.; Alivisatos, A. P. *Adv. Mater.* **1999**, *11*, 923-927.
- (2) Hikmet, R. A. M.; Talapin, D. V.; Weller, H. *J. Appl. Phys.* **2003**, *93*, 3509-3514.
- (3) Han, M. Y.; Gao, X. H.; Su, J. Z.; Nie, S. *Nat. Biotechnol.* **2001**, *19*, 631-635.
- (4) Sandros, M. G.; Shete, V.; Benson, D. E. *Analyst* **2006**, *131*, 229-235.
- (5) Peng, X. G.; Schlamp, M. C.; Kadavanich, A. V.; Alivisatos, A. P. *J. Am. Chem. Soc.* **1997**, *119*, 7019-7029.
- (6) Hines, M. A.; Guyot-Sionnest, P. *J. Phys. Chem.* **1996**, *100*, 468-471.
- (7) Huynh, W. U.; Dittmer, J. J.; Alivisatos, A. P. *Science* **2002**, *295*, 2425-2427.
- (8) Ivanov, S. A.; Nanda, J.; Piryatinski, A.; Achermann, M.; Balet, L. P.; Bezel, I. V.; Anikeeva, P. O.; Tretiak, S.; Klimov, V. I. *J. Phys. Chem. B* **2004**, *108*, 10625-10630.
- (9) Zegrya, G. G.; Andreev, A. D. *Appl. Phys. Lett.* **1995**, *67*, 2681-2683.
- (10) Ivanov, S. A.; Piryatinski, A.; Nanda, J.; Tretiak, S.; Zavadil, K. R.; Wallace, W. O.; Werder, D.; Klimov, V. I. *J. Am. Chem. Soc.* **2007**, *129*, 11708-11719.
- (11) Oron, D.; Kazes, M.; Banin, U. *Phys. Rev. B* **2007**, *75*, 035330.
- (12) Klimov, V. I.; Schwarz, C. J.; McBranch, D. W.; Leatherdale, C. A.; Bawendi, M. G. *Phys. Rev. B* **1999**, *60*, R2177-R2180.
- (13) Klimov, V. I.; Mikhailovsky, A. A.; Xu, S.; Malko, A.; Hollingsworth, J. A.; Leatherdale, C. A.; Eisler, H. J.; Bawendi, M. G. *Science* **2000**, *287*, 1011-1013.
- (14) Chen, C. Y.; Cheng, C. T.; Lai, C. W.; Hu, Y. H.; Chou, P. T.; Chou, Y. H.; Chiu, H. T. *Small* **2005**, *1*, 1215-1220.
- (15) Cheng, C. T.; Chen, C. Y.; Lai, C. W.; Liu, W. H.; Pu, S. C.; Chou, P. T.; Chou, Y. H.; Chiu, H. T. *J. Mater. Chem.* **2005**, *15*, 3409-3414.
- (16) Xie, R. G.; Zhong, X. H.; Basche, T. *Adv. Mater.* **2005**, *17*, 2741-2744.
- (17) Kim, S.; Fisher, B.; Eisler, H. J.; Bawendi, M. G. *J. Am. Chem. Soc.* **2003**, *125*, 11466-11467.
- (18) Klimov, V. I.; Ivanov, S. A.; Nanda, J.; Achermann, M.; Bezel, I.; McGuire, J. A.; Piryatinski, A. *Nature* **2007**, *447*, 441-446.
- (19) Balet, L. P.; Ivanov, S. A.; Piryatinski, A.; Achermann, M.; Klimov, V. I. *Nano Lett.* **2004**, *4*, 1485-1488.

(20) Shim, M.; Guyot-Sionnest, P. *J. Am. Chem. Soc.* **2001**, *123*, 11651–11654.

(21) Ouyang, J. Y.; Ratcliffe, C. I.; Kingston, D.; Wilkinson, B.; Kuijper, J.; Wu, X. H.; Ripmeester, J. A.; Yu, K. *J. Phys. Chem. C* **2008**, *112*, 4908–4919.

(22) Weinhardt, L.; Heske, C.; Umbach, E.; Niesen, T. P.; Visbeck, S.; Karg, F. *Appl. Phys. Lett.* **2004**, *84*, 3175–3177.

(23) Son, D. H.; Hughes, S. M.; Yin, Y. D.; Alivisatos, A. P. *Science* **2004**, *306*, 1009–1012.

(24) Wong, E. M.; Searson, P. C. *Appl. Phys. Lett.* **1999**, *74*, 2939–2941.

(25) Rorison, J. M. *Phys. Rev. B* **1993**, *48*, 4643–4649.

(26) Felix, C. L.; Bewley, W. W.; Vurgaftman, I.; Meyer, J. R.; Zhang, D.; Lin, C. H.; Yang, R. Q.; Pei, S. S. *IEEE Photon Technol. Lett.* **1997**, *9*, 1433–1435.

(27) Sajinovic, D.; Saponjic, Z. V.; Cvjeticanin, N.; Marinovic-Cincovic, M.; Nedeljkovic, J. M. *Chem. Phys. Lett.* **2000**, *329*, 168–172.

JP903813H